
Exploring Hidden Dimensions in Parallelizing Convolutional Neural Networks

Zhihao Jia¹ Sina Lin² Charles R. Qi¹ Alex Aiken¹

Abstract

The past few years have witnessed growth in the size and computational requirements for training deep convolutional neural networks. Current approaches parallelize the training process onto multiple devices by applying a single parallelization strategy (e.g., data or model parallelism) to all layers in a network. Although easy to reason about, this design results in suboptimal runtime performance in large-scale distributed training, since different layers in a network may prefer different parallelization strategies. In this paper, we propose *layer-wise parallelism* that allows each layer in a network to use an individual parallelization strategy. We jointly optimize how each layer is parallelized by solving a graph search problem. Our experiments show that layer-wise parallelism outperforms current parallelization approaches by increasing training speed, reducing communication costs, achieving better scalability to multiple GPUs, while maintaining the same network accuracy.

1. Introduction

Convolutional neural networks (CNNs) have proven to be general and effective across many tasks including image classification (Krizhevsky et al., 2012; Szegedy et al., 2016), face recognition (Lawrence et al., 1997), text classification (Wang et al., 2012), and game playing (Silver et al., 2016). Their success has resulted in growth in the size and computational requirements to train deep CNNs. It takes days or even weeks to train a deep CNN from scratch (Szegedy et al., 2014; Zeiler & Fergus, 2014; Simonyan & Zisserman, 2014; Szegedy et al., 2016).

There has been a large number of research work on parallelization and distribution techniques to speed up the training process. The most common parallelization technique is *data parallelism* (Krizhevsky et al., 2012; Simonyan & Zisserman, 2014) that divides the entire training dataset

into same-sized batches and assigns each batch to a single device. Another possible approach to parallelize CNNs is *model parallelism* (Mirhoseini et al., 2017; Kim et al., 2017) that divides the network parameters into disjoint subsets and trains each subset on a dedicated device. Both parallelization approaches apply a single parallelization strategy (i.e., data or model parallelism) to all layers in a CNN. However, within a CNN, different layers may prefer different parallelization strategies for achieving optimal runtime performance. For example, a densely-connected layer with millions of parameters prefers model parallelism to reduce communication cost for synchronizing parameters, while a convolutional layer typically prefers data parallelism to eliminate data transfers from the previous layer. In addition, some layers may prefer more sophisticated parallelization strategies such as parallelizing a layer in a mixture of multiple data dimensions (see Section 3). Because of the preference diversity among different layers in a network, applying a single parallelization strategy to all layers may result in suboptimal runtime performance.

In this paper, we propose *layer-wise parallelism*, which allows each layer in a network to use an individual parallelization strategy. Layer-wise parallelism performs the same computation for each layer as it is defined in the original network and therefore maintains the same network accuracy by design. Compared to existing parallelization approaches, our approach defines a more comprehensive search space for parallelizing a network, which includes data and model parallelism as two special cases. Our goal is to find the parallelization strategies for individual layers to jointly achieve the best possible runtime performance while maintaining the original network accuracy. To formalize the problem, we introduce *parallelism configurations* that define the search space for parallelizing a layer across multiple devices. We propose a cost model that quantitatively evaluates the runtime performance of different parallelism configurations. The cost model considers both the computation power of each device and the communication bandwidth between devices. With the cost model, we convert the original problem of assigning parallelism configurations to individual layers to a graph search problem and develop an efficient algorithm to find a globally optimal parallelization.

We test layer-wise parallelism with AlexNet (Krizhevsky et al., 2012), VGG-16 (Simonyan & Zisserman, 2014), and

¹Stanford University ²Microsoft. Correspondence to: Zhihao Jia <zhihao@cs.stanford.edu>.

Inception-v3 (Szegedy et al., 2016) on the ILSVRC 2012 dataset (Deng et al., 2009) for 1000-class image classification. For distributed training on 16 GPUs, layer-wise parallelism achieves 1.5 - 2.9 \times speedup over other parallelization approaches. Note that the speedup is achieved without losing the network accuracy, since layer-wise parallelism trains the same network as data and model parallelism and uses a more sophisticated parallelization strategy to achieve better runtime performance. In addition, layer-wise parallelism also reduces communication costs by 1.3 - 23.0 \times compared to data and model parallelism. Finally, we show that layer-wise parallelism achieves better scalability than other parallelization approaches. Scaling the training of Inception-v3 from 1 GPU to 16 GPUs, layer-wise parallelism obtains 15.5 \times speedup, while other parallelization approaches get at most 11.2 \times speedup.

The main contributions of this paper are:

- We propose layer-wise parallelism that allows different layers in a network to use individual parallelism configurations.
- We formally define the search space of all possible parallelism configurations for a layer and present a cost model to quantitatively evaluate the runtime performance of training a network. Based on the cost model, we develop an efficient algorithm to jointly find a globally optimal parallelization.
- We provide an implementation that supports layer-wise parallelism and show that, in a set of realistic CNN benchmarks, layer-wise parallelism significantly increases training speed, reduces communication costs and improves scalability compared to state-of-the-art parallelization approaches.

2. Related Work

Data and model parallelism. Data parallelism has been widely used by existing deep learning frameworks (e.g., TensorFlow (Abadi et al., 2016), Caffe2², and PyTorch³) to distribute the training process onto multiple devices by assigning each device a subset of the training data. The standard data parallelism strategy keeps a copy of the entire neural network on each device, which is a scalability bottleneck for large scale distributed training.

Mirhoseini et al. (2017) uses model parallelism to assign each layer in a network to a dedicated device and uses a reinforcement learning algorithm to optimize the placement of each layer on a GPU device. Kim et al. (2017) proposes a network design that splits the network parameters into multiple disjoint subsets and assigns each subset to one device,

which allows different devices to train disjoint subsets of network parameters. Model parallelism reduces communication costs for synchronizing the network parameters but exposes limited parallelism for large scale training.

Krizhevsky (2014) introduces “one weird trick” (OWT) that uses data parallelism for parallelizing convolutional layers and switches to model parallelism for parallelizing fully-connected layers. This contribution reduces the data transfer costs of data parallelism. In this paper, we use OWT parallelism as a baseline in our experiments and show that layer-wise parallelism can further reduce communication and improve speedup compared to OWT parallelism.

System optimizations. A number of system-level optimizations have been proposed to accelerate large scale training. Goyal et al. (2017) empirically shows no loss of accuracy for training ResNet-50 on 256 GPUs with a very large batch size using a three-step allreduce operation to optimize communication across devices and aggressively overlapping gradient synchronization with back propagation. Zhang et al. (2017) introduces a hybrid communication scheme that reduces communication costs for gradient synchronization in each layer. All these systems are based on data parallelism and are limited in runtime performance by communication costs.

Network parameter reduction. Recently, parameter reduction techniques have been proposed to reduce communication in large scale training. Han et al. (2015) presents an iterative weight pruning method that repeatedly retrains the network while removing weak connections. Alvarez & Salzmann (2016) proposes a network that learns the redundant parameters in each layer and iteratively eliminates the redundant parameters. These approaches improve runtime performance by significantly reducing the number of parameters in a neural network, which results in a modified network and may decrease the network accuracy (as reported in these papers). By contrast, in this paper, we introduce a new parallelization approach that accelerates distributed learning while training the original network.

3. Hidden Dimensions in Parallelizing a Layer

Data parallelism parallelizes the training of CNNs by giving each device a subset of the images. However, other dimensions can be used to parallelize the training process. For example, in standard CNNs for 2D images, data is commonly organized as 4-dimensional tensors (i.e., image, height, width, channel). The *image* dimension includes an index for each image in the input dataset. The *height* and *width* dimensions specify a position in an image. For a particular position, the *channel* dimension indexes different neurons for that position.

In principle, any combination of these dimensions can be used to parallelize a layer, and we should consider both

²<https://caffe2.ai>

³<https://pytorch.org>

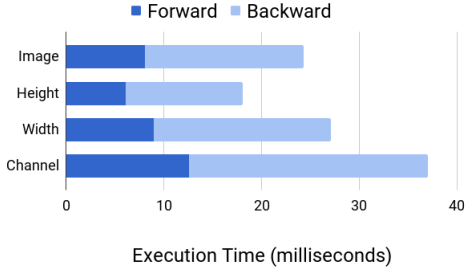
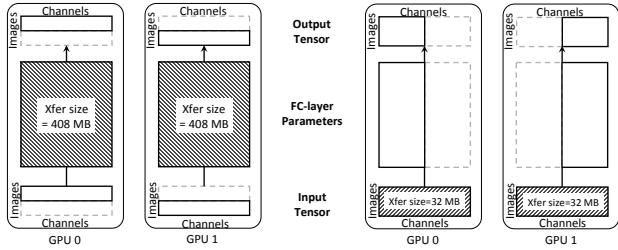


Figure 1. Execution time for processing a convolutional layer (Conv8 in VGG-16 (Simonyan & Zisserman, 2014)) on 4 GPUs by using parallelism in different dimensions. Parallelizing a convolutional layer in other dimensions preserves the same output as parallelizing it in the image dimension. To achieve this, different GPUs may share some common input data for parallelizations in the height, width, and channel dimensions.



(a) Parallelism in the image dimension.

(b) Parallelism in the channel dimension.

Figure 2. Different ways to parallelize the first fully-connected layer of VGG-16. Rectangles with solid lines indicate tensors managed by the local GPU, while rectangles with dotted lines are tensors managed by a remote GPU. The shadow rectangles indicate data transfers in each step.

selecting the dimensions to be parallelized and the degree of parallelism in each dimension. Exploring these additional dimensions has the following advantages.

First, parallelizing a layer in other dimensions can reduce execution time. Figure 1 shows the time to process a 2D convolutional layer on 4 GPUs using parallelism in different dimensions. The figure shows that image parallelism is not always the best choice.

Second, exploring parallelism in other dimensions can reduce communication costs. Figure 2 shows an example of parallelizing a fully-connected layer on two GPUs in different dimensions. In data parallelism (Figure 2a), each GPU synchronizes the gradients of the entire fully-connected layer (shown as the shadow rectangles) in every step. An alternative approach (Figure 2b) parallelizes in the channel dimension by assigning a subset of the output channels to each GPU. As a result, different GPUs train disjoint subsets of the fully-connected layer, which eliminates transferring the fully-connected layer but introduces additional data transfers for input tensors (shown as the shadow rectangles). For this particular case, using parallelism in the channel

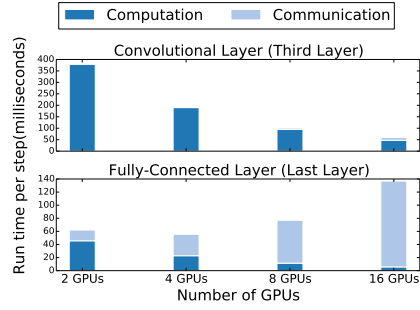


Figure 3. Computation and communication time to process the third layer and the last layer of Inception-v3 using data parallelism.

Table 1. Parallelizable dimensions for different layers. The length dimension specify a position in a 1D image.

Layer	Parallelizable dimensions
Fully-connected	{image, channel}
1D convolution	{image, channel, length}
2D convolution	{image, channel, height, width}
3D convolution	{image, channel, height, width, depth}

dimension reduces communication by $12\times$.

Third, the *degree* of parallelism (number of parallel devices) is another dimension that affects runtime performance. Different layers within a neural network have different execution time and communication costs and so may prefer different degrees of parallelism. Figure 3 shows the runtime performance of processing two layers in Inception-v3 with different degrees of parallelism. The convolutional layer performs best on 16 GPUs, while the fully-connected layer performs best on 4 GPUs.

4. Problem Definition

We define the parallelization problem with two graphs. The first is a *device graph* that models all available hardware devices and the connections between them. The second is a *computation graph* that defines the neural network to be mapped onto the device graph.

In the device graph $\mathcal{G}_D = (\mathcal{D}, \mathcal{B})$, each node $d_i \in \mathcal{D}$ is a device (e.g., a CPU or a GPU), and each edge $(d_i, d_j) \in \mathcal{B}$ represents an connection between device d_i and d_j with communication bandwidth $b(d_i, d_j)$. In the computation graph $\mathcal{G} = (\mathcal{N}, \mathcal{E})$, each node $n_i \in \mathcal{N}$ is a layer in the neural network, and each edge $(n_i, n_j) \in \mathcal{E}$ is a tensor that is an output of layer n_i and an input of layer n_j .

We now define the parallelism of a layer n_i . To allow parallelization among multiple devices, we assume that different devices can process the same layer in parallel without any dependencies. This requires different devices to compute *disjoint* subsets of the layer’s output tensors. Therefore, we describe the parallelism of a layer n_i by defining how the output tensor of n_i is partitioned.

For a layer n_i , we define its *parallelizable dimensions* \mathcal{P}_i

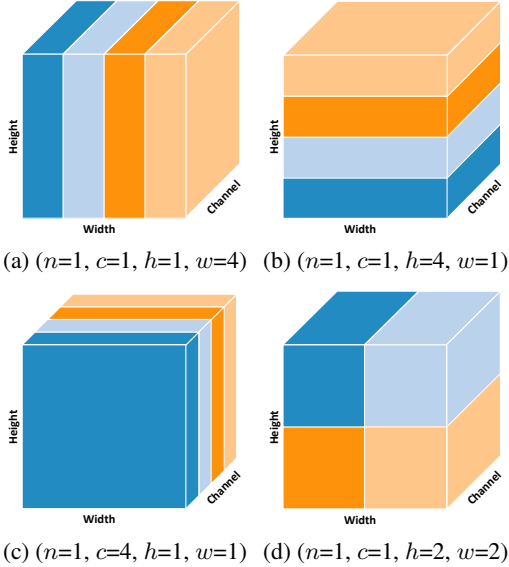


Figure 4. Example parallelism configurations that parallelize a 2D convolutional layer in a single dimension or combinations of multiple dimensions. The figure shows how each image is partitioned in different configurations.

as the set of all divisible dimensions in its output tensor. \mathcal{P}_i includes all dimensions to parallelize the layer n_i . Table 1 shows the parallelizable dimensions for some layers.

A *parallelism configuration* c_i of a layer n_i defines how n_i is parallelized across different devices. For each parallelizable dimension in \mathcal{P}_i , c_i includes a positive integer that describes the degree of parallelism in that dimension. For a parallelism configuration c_i , the product of the integers over all dimensions is the total degree of parallelism for n_i . We assume equal partitioning in each parallelizable dimension, which provides well-balanced work among multiple devices. Figure 4 demonstrates some possible parallelism configurations for parallelizing a 2D convolutional layer over 4 devices. For a layer n_i , parallelizing the layer in any parallelism configuration c_i produces the same output. This guarantees that all configurations parallelize the training process on the original network and therefore maintains the original network accuracy.

A *global configuration* \mathcal{C} includes a parallelism configuration c_i for each layer $n_i \in \mathcal{N}$. Let $t(\mathcal{G}, \mathcal{C})$ denote the execution time to perform one step of the training process for computation graph \mathcal{G} under the global configuration \mathcal{C} . The goal of *parallelism optimization* problem is to find \mathcal{C} such that the per-step training time $t(\mathcal{G}, \mathcal{C})$ is minimized.

5. Method

5.1. Cost Model for Parallelism Configurations

We introduce a cost model that quantitatively estimates the performance of different parallelism configurations and translates the original problem into a global search problem. Af-

ter that, we present an efficient graph algorithm to find the optimal global configuration by solving the global search problem.

Our method depends on the following assumptions:

1. For a layer $n_i \in \mathcal{N}$, the time to process n_i is predictable with low variance.
2. For each connection (d_i, d_j) between device d_i and d_j with bandwidth b , transferring a tensor of size s from d_i to d_j takes s/b time (i.e., the communication bandwidth can be fully utilized).
3. The runtime system has negligible overhead. A device begins processing a layer as soon as its input tensors are available, and there are no other active layers on that device.

We verify the first assumption in the supplementary materials, and the experiments show that our implementation satisfies the second and third assumptions well enough to obtain significant runtime performance improvements.

We define three cost functions:

1. For each node n_i and its parallelism configuration c_i , $t_C(n_i, c_i)$ is the time to process the layer n_i under the parallelism configuration c_i . This includes both the forward and back propagation time and is estimated by running the layer under that configuration multiple times on the device and measuring the average execution time.
2. For each edge $e = (n_i, n_j) \in \mathcal{E}$, $t_X(e, c_i, c_j)$ estimates the time to transfer the input tensors to the target devices, using the size of the data to be moved and the known communication bandwidth. Note that $t_X(e, c_i, c_j)$ is zero if c_i and c_j have the same parallelism configuration (i.e., $c_i = c_j$), in which case no data is transferred.
3. For each node n_i and its parallelism configuration c_i , $t_S(n_i, c_i)$ estimates the time to synchronize the parameters for layer n_i after back propagation. To complete parameter synchronization, each device that holds a copy of the parameters for layer n_i transfers its local gradients to a parameter server that stores the up-to-date parameters for layer n_i . After receiving the gradients for layer n_i , the parameter server applies the gradients to the parameters and transfers the updated parameters back to the device. In this process, the communication time is much longer than the execution time to update parameters, therefore we use the communication time to approximate the parameter synchronization time.

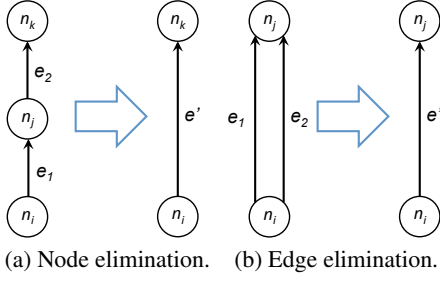


Figure 5. Perform a node/edge elimination on a computation graph.

Using the three cost functions above, we define

$$t_O(\mathcal{G}, \mathcal{C}) = \sum_{n_i \in \mathcal{N}} \{t_C(n_i, c_i) + t_S(n_i, c_i)\} + \sum_{e=(n_i, n_j) \in \mathcal{E}} t_X(e, c_i, c_j) \quad (1)$$

$t_O(\mathcal{G}, \mathcal{C})$ estimates the per-step execution time under global configuration \mathcal{C} . This execution time includes forward processing, back propagation, and parameter synchronization.

5.2. Graph Algorithm

Equation 1 expresses the problem of finding an optimal global configuration as a graph search problem: our goal is to find a global configuration \mathcal{C} that includes a parallelism configuration c_i for each node $n_i \in \mathcal{N}$ so that the global cost $t_O(\mathcal{G}, \mathcal{C})$ is minimized.

The number of potential global configurations is exponential in the number of nodes in a computation graph, which makes it impractical to enumerate all global configurations for large CNNs. However, the CNNs we have seen in practice exhibit strong locality: each node is only connected to a few nodes with similar depths in a computation graph. Based on this observation, we use the following two graph operations to iteratively simplify the computation graph while preserving the optimal global configuration.

Node elimination. In a computation graph \mathcal{G} , if \mathcal{G} includes a node n_j with a single in-edge $e_1 = (n_i, n_j)$ and a single out-edge $e_2 = (n_j, n_k)$, a node elimination removes node n_j and the two edges e_1 and e_2 from \mathcal{G} , inserts a new edge $e' = (n_i, n_k)$ back into \mathcal{G} , and returns the modified graph (Figure 5a). We define $t_X(e', \cdot, \cdot)$ in a way that preserves the optimal global configuration (see Theorem 1).

$$t_X(e', c_i, c_k) = \min_{c_j} \{t_C(n_j, c_j) + t_S(n_j, c_j) + t_X(e_1, c_i, c_j) + t_X(e_2, c_j, c_k)\} \quad (2)$$

Intuitively, we use dynamic programming to compute the optimal configuration c_j for node n_j for every possible combination of c_i and c_k and use the cost functions associated with n_j to define $t_X(e', c_i, c_k)$.

Algorithm 1 Finding Optimal Global Configuration \mathcal{C} .

```

1: Input:  $\mathcal{G}_D = (\mathcal{D}, \mathcal{B})$ ,  $\mathcal{G} = (\mathcal{N}, \mathcal{E})$ , precomputed  $t_C(\cdot)$ 
   and  $t_S(\cdot)$  for  $\forall n_i \in \mathcal{N}$  and  $t_X(\cdot)$  for  $\forall e \in \mathcal{E}$ 
2: Output: A global configuration  $\mathcal{C}$  minimizing  $t_O(\mathcal{G}, \mathcal{C})$ 
3:
4:  $\mathcal{G}^{(0)} = \mathcal{G}$ 
5:  $m = 0$ 
6: while true do
7:    $\mathcal{G}^{(m+1)} = \text{NODEELIMINATION}(\mathcal{G}^{(m)})$ 
8:    $\mathcal{G}^{(m+2)} = \text{EDGEELIMINATION}(\mathcal{G}^{(m+1)})$ 
9:   if  $\mathcal{G}^{(m+2)} = \mathcal{G}^{(m)}$  then
10:    break
11:   end if
12:    $m = m + 2$ 
13: end while
14: Find optimal  $\mathcal{C}^{(m)}$  for  $\mathcal{G}^{(m)}$  by enumerating all possible
   configurations for  $\mathcal{G}^{(m)}$ 
15: for  $i = m-1$  to 0 do
16:   if  $\mathcal{G}^{(i+1)} = \text{NODEELIMINATION}(\mathcal{G}^{(i)})$  then
17:      $\triangleright$  Assume  $n_j$  is the node eliminated from  $\mathcal{G}^{(i)}$ 
18:     Find  $c_j$  that minimizes Equation 1
19:      $\mathcal{C}^{(i)} = \mathcal{C}^{(i+1)} + c_j$ 
20:   else
21:      $\mathcal{C}^{(i)} = \mathcal{C}^{(i+1)}$ 
22:   end if
23: end for
24: return  $\mathcal{C}^{(0)}$ 
    
```

Theorem 1. Assume $\mathcal{G}' = \text{NodeElimination}(\mathcal{G})$ and n_j is the eliminated node. If \mathcal{C}_o' is an optimal global configuration of \mathcal{G}' , then $\mathcal{C}_o = \mathcal{C}_o' + c_j$ is an optimal global configuration of \mathcal{G} , where c_j minimizes Equation 2.

Edge elimination. If a computation graph \mathcal{G} includes two edges with the same source and destination node (i.e., $e_1 = (n_i, n_j)$ and $e_2 = (n_i, n_j)$), an edge elimination removes e_1 and e_2 from \mathcal{G} , inserts a new edge $e' = (n_i, n_j)$ into \mathcal{G} (Figure 5b). We define $t_X(e', \cdot, \cdot)$ using $t_X(e_1, \cdot, \cdot)$ and $t_X(e_2, \cdot, \cdot)$.

$$t_X(e', c_i, c_j) = t_X(e_1, c_i, c_j) + t_X(e_2, c_i, c_j) \quad (3)$$

Theorem 2. Assume $\mathcal{G}' = \text{EdgeElimination}(\mathcal{G})$, and \mathcal{C}_o' is an optimal global configuration of \mathcal{G}' , then \mathcal{C}_o' is also an optimal global configuration of \mathcal{G} .

We formally define node and edge eliminations and prove Theorem 1 and 2 in the supplementary materials. The two theorems show that given an optimal global configuration for the modified graph, we can easily construct an optimal global configuration for the original graph.

Algorithm 1 shows pseudocode using node and edge eliminations as subroutines to find the optimal global configuration. The algorithm first iteratively uses node and edge

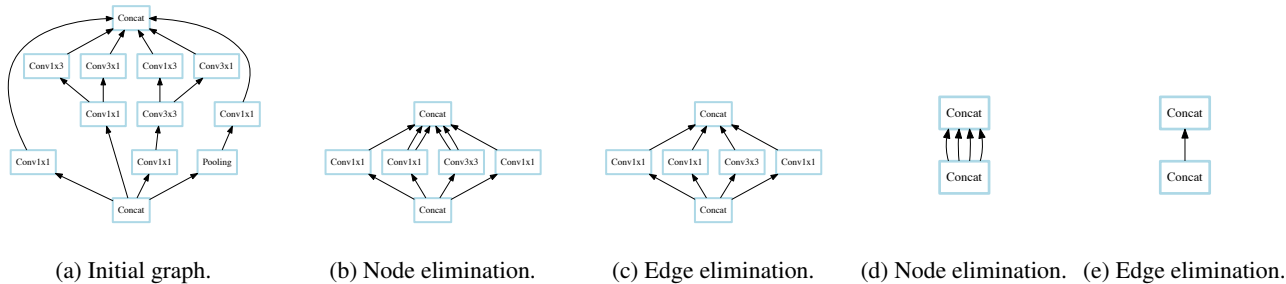


Figure 6. Iteratively performing node/edge eliminations on an Inception module.

Table 2. Time complexity of the graph algorithm. C is the maximum number of possible parallelism configurations for a layer. N and E are the size of \mathcal{N} and \mathcal{E} , respectively. K is the number of nodes in the final graph after node and edge eliminations.

Step	Time Complexity
Performing node and edge eliminations	$O(EC^3)$
Finding an optimal configuration for the final graph	$O(KC^K)$
Undoing node and edge eliminations	$O(EC)$
Overall	$O(EC^3 + KC^K)$

eliminations to simplify the computation graph until neither elimination can be applied (lines 4-13). Figure 6 shows how the algorithm iteratively performs node and edge eliminations for a complex Inception module (Szegedy et al., 2016).

After the elimination phase, the algorithm enumerates all global configurations for the final graph $\mathcal{G}^{(m)}$ and chooses $\mathcal{C}^{(m)}$ that minimizes $t_o(\mathcal{G}^{(m)}, \mathcal{C}^{(m)})$ (line 14). After deciding the configuration for each node in $\mathcal{G}^{(m)}$, we then decide the configurations for the eliminated nodes by undoing the node and edge eliminations in reverse order (lines 15-23). Theorem 1 and 2 guarantee that $\mathcal{C}^{(i)}$ is an optimal global configuration for $\mathcal{G}^{(i)}$ ($0 \leq i \leq m$). Finally, $\mathcal{C}^{(0)}$ is an optimal global configuration for the original graph \mathcal{G} .

Time complexity. Table 2 shows the time complexity of our algorithm. Performing a node or edge elimination requires computing Equation 2 or 3 for the inserted edge, which takes $O(C^3)$ and $O(C^2)$ time, respectively. The total number of node and edge eliminations is smaller than E , since an elimination reduces the number of edges in the graph by one. Therefore, the time complexity for performing and undoing node and edge eliminations is $O(EC^3)$ and $O(EC)$, respectively. The algorithm enumerates all global configurations for the final graph $\mathcal{G}^{(m)}$ to find an optimal configuration, which takes $O(KC^K)$ time. We find that the algorithm works efficiently on a wide range of real-world CNNs including AlexNet (Krizhevsky et al., 2012), VGG-16 (Simonyan & Zisserman, 2014), Inception-v3 (Szegedy et al., 2016), and ResNet (He et al., 2016), all of which are reduced to a final graph with only 2 nodes (i.e., $K = 2$).

Table 3. Execution time for finding the optimal global configuration with 4 GPUs. Note that the number of nodes in the final graph (i.e., K) is equal to 2 for all networks.

Network	# Layers	Baseline	Our Algorithm
LeNet-5	6	5.6 seconds	0.01 seconds
AlexNet	11	2.1 hours	0.02 seconds
VGG-16	21	> 24 hours	0.1 seconds
Inception-v3	102	> 24 hours	0.4 seconds
Time complexity		$O(EC^N)$	$O(EC^3)$

We compare Algorithm 1 with a baseline algorithm that uses a *depth-first search* algorithm to find the optimal global configuration in the original graph \mathcal{G} . Table 3 compares the time complexity and actual execution time of the two algorithms. Our algorithm achieves lower time complexity and reduces the execution time to find the optimal global configuration by orders of magnitude over the baseline.

6. Experiments

We describe implementation details in the supplementary materials. In the experiments, we compare the runtime performance of layer-wise parallelism against state-of-the-art baselines described in Section 2.

Benchmarks. We evaluate our algorithm on three established convolutional neural networks. AlexNet (Krizhevsky et al., 2012) includes 5 convolutional layers and 3 fully-connected layers and was the winner of the ILSVRC-2012 competition. VGG-16 (Simonyan & Zisserman, 2014) achieves performance improvement by pushing the depth of the network to 16 weighted layers. Inception-v3 (Szegedy et al., 2016) is a 102-layer deep CNN that uses carefully designed Inception modules to increase the number of layers while maintaining a reasonable computational budget.

Datasets. We evaluate all three CNN benchmarks on the ImageNet-1K dataset (Deng et al., 2009) that consists of 1.2 million images from 1,000 categories.

Baselines. We compare the following parallelization approaches in the experiments.

1. **Data parallelism** is the most common parallelization approach used in large-scale CNN training. In data parallelism, each device has a copy of the entire network and processes disjoint subsets of the training data.
2. **Model parallelism.** We use a model parallelism approach (Krizhevsky, 2014) as a baseline, which distributes the parameters in each layer equally to all devices, providing good load balancing.
3. **OWT parallelism** is designed to reduce communication costs in distributed CNN training by using data parallelism for training convolutional layers and pooling layers and switching to model parallelism for training fully-connected layers.
4. **Layer-wise parallelism.** Given a benchmark network and a set of available devices, we run the algorithm described in Section 5 to find the optimal global configuration \mathcal{C} and parallelize each layer n_i by using the discovered parallelism configuration $c_i \in \mathcal{C}$.

Experimental setup. All experiments were performed on a GPU cluster with 4 machines, each of which is equipped with two Intel 10-core E5-2600 CPUs, 256G main memory, and four NVIDIA Tesla P100 GPUs. GPUs on the same machine are connected by NVLink, and machines are connected over 100Gb/s EDR Infiniband. We use synchronous training and a batch size of 32 for all experiments. We run data parallelism experiments in TensorFlow r1.4, PyTorch v0.3, and our implementation and report the best runtime performance number of the three. All other experiments were performed using our implementation, which uses the Legion task-based runtime (Bauer et al., 2012).

6.1. Runtime Performance Comparison

We compare the training throughput and communication cost among different parallelization approaches. Figure 7 shows the training throughputs with different CNNs and different sets of available devices. Both model and data parallelism scale well in a single node but show limited scalability in distributed training, where the inter-node communication limits runtime performance. OWT parallelism achieves improved runtime performance by switching to model parallelism for fully-connected layers to reduce data transfers. In layer-wise parallelism, we first find the optimal global configuration for a given CNN and a given set of available devices and then use the discovered configuration to parallelize the training process. In all experiments, layer-wise parallelism consistently outperforms the other baseline parallelization approaches and achieves up to $2.9\times$, $1.8\times$, and $1.5\times$ speedup for AlexNet, VGG-16, and Inception-v3, compared to data parallelism.

In addition, layer-wise parallelism achieves better scalability

Table 4. Relative difference between estimated execution time $t_o(\mathcal{G}, \mathcal{C})$ and actual execution time $t(\mathcal{G}, \mathcal{C})$.

Available Devices	$(t_o(\mathcal{G}, \mathcal{C}) - t(\mathcal{G}, \mathcal{C})) / t(\mathcal{G}, \mathcal{C})$		
	AlexNet	VGG-16	Inception-v3
1 GPU (1 node)	1%	0%	1%
2 GPUs (1 node)	4%	3%	5%
4 GPUs (1 node)	-5%	2%	5%
8 GPUs (2 nodes)	2%	6%	9%
16 GPUs (4 nodes)	-1%	7%	6%

than the other approaches. Scaling the training of the three networks from 1 GPU to 16 GPUs on 4 machines, layer-wise parallelism achieves $12.2\times$, $14.8\times$, and $15.5\times$ speedup for AlexNet, VGG-16, and Inception-v3, respectively, while the best other parallelization approach achieves $6.1\times$, $10.8\times$, and $11.2\times$ speedup. Moreover, Figure 7 shows that the layer-wise parallelism can help bridge the runtime performance gap between the ideal training throughputs in linear scale (the red lines) and the actual training throughputs achieved by current parallelization approaches. This shows that layer-wise parallelism is more efficient for parallelizing large-scale training.

Communication cost is another important performance metric in large-scale training. We compare the communication cost among different parallelization approaches in Figure 8. The OWT parallelism approach, which is designed to optimize data transfers, reduces the communication cost by $1.1 - 23.0\times$ compared to data and model parallelism. Layer-wise parallelism outperforms OWT parallelism by further reducing the communication overhead by $1.2 - 2.5\times$.

6.2. Estimated Execution Time $t_o(\mathcal{G}, \mathcal{C})$

We compare the estimated execution time $t_o(\mathcal{G}, \mathcal{C})$ projected by our cost model (see Equation 1) with the measured per-step execution time $t(\mathcal{G}, \mathcal{C})$ in the experiments. The results are shown in Table 4. In all experiments, the relative difference between the estimated and the real execution time is within 10%, showing our cost model can reliably predict a CNN’s per-step execution time given the set of available devices and the connections between them. Therefore, we believe that our model is useful for choosing the set of available devices for achieving optimal runtime performance.

6.3. Analysis of Optimal Configurations

We analyze the optimal global configurations and find several similarities among them.

First, for the beginning layers of a CNN with large height/width dimensions and a small channel dimension, the optimal configuration usually uses data parallelism on all available devices, since the communication cost for synchronizing gradients is much smaller than the communication cost for moving tensors between layers.

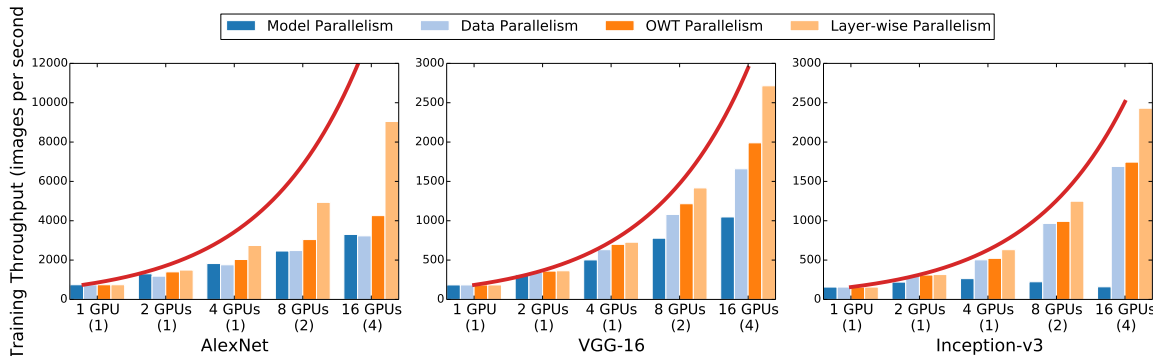


Figure 7. Training throughput (i.e., number of images trained per second) for parallelizing different networks (higher is better). Numbers in parenthesis are the number of machines used in the experiments. The red lines show the training throughput in linear scale (ideal case).

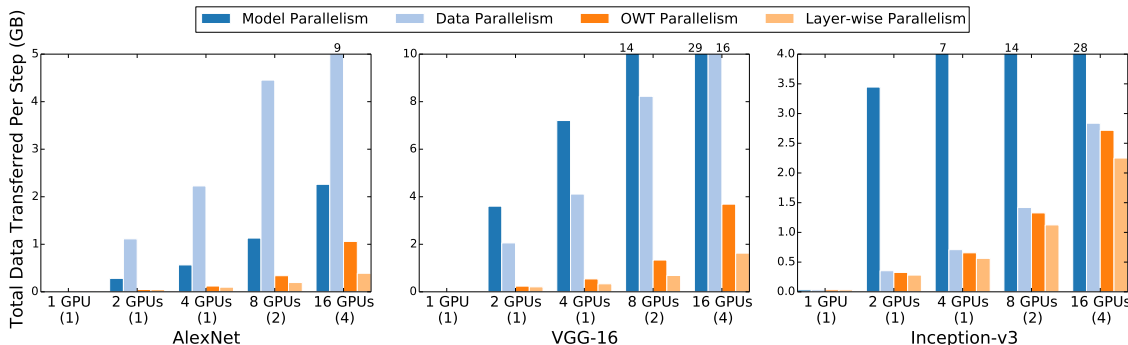


Figure 8. Communication cost (i.e., data transferred in each step) for parallelizing different networks (lower is better).

Table 5. The optimal global configuration for training VGG-16 on 4 GPUs.

Layers	Parallelism Configuration
2 x Conv + Pooling	{n=4, h=1, w=1, c=1}
2 x Conv + Pooling	
3 x Conv + Pooling	
3 x Conv + Pooling	
3 x Conv + Pooling	{n=1, h=2, w=2, c=1}
Fully-connected	{n=1, c=4}
Fully-connected	
Fully-connected	{n=1, c=2}
Softmax	{n=1, c=1}

Second, deeper layers in a CNN tend to have smaller height/width dimensions and a larger channel dimension. As a result, the cost for moving tensors between different layers decreases, while the cost for synchronizing parameters increases. The optimal configuration adaptively reduces the number of devices for these layers to reduce the communication cost for synchronizing parameters and may use parallelism in the height/width dimensions to achieve better runtime performance.

Third, the optimal configuration eventually switches to model parallelism on a small number of devices for fully-connected layers, because synchronizing gradients and moving tensors are both much more expensive than the compute time for fully-connected layers. This reduces the communi-

cation cost for synchronizing parameters and moving tensors at the cost of a smaller degree of parallelism.

Table 5 shows the optimal global configuration for training VGG-16 on 4 GPUs on a single node. The optimal configuration first uses parallelism in the image dimension for the beginning convolutional and pooling layers and then uses parallelism in both the height and width dimensions to accelerate the last three convolutional layers. For the fully-connected layers, the optimal configuration uses parallelism in the channel dimension to reduce communication cost and decreases the degree of parallelism.

7. Conclusion

We have introduced layer-wise parallelism, which allows each layer in a network to use an individual parallelization configuration. We proposed a cost model that quantitatively evaluates the runtime performance of different parallelism configurations and presented an efficient algorithm to find a globally optimal parallelization by solving a graph search problem. Our experiments show that layer-wise parallelism significantly outperforms state-of-the-art parallelization approaches for CNNs by increasing training speed, reducing communication costs, and achieving better scalability on larger numbers of devices. We are planning to open source our algorithm and system implementation to facilitate further study and research.

References

- Abadi, Martín, Barham, Paul, Chen, Jianmin, Chen, Zhifeng, Davis, Andy, Dean, Jeffrey, Devin, Matthieu, Ghemawat, Sanjay, Irving, Geoffrey, Isard, Michael, Kudlur, Manjunath, Levenberg, Josh, Monga, Rajat, Moore, Sherry, Murray, Derek G., Steiner, Benoit, Tucker, Paul, Vasudevan, Vijay, Warden, Pete, Wicke, Martin, Yu, Yuan, and Zheng, Xiaoqiang. Tensorflow: A system for large-scale machine learning. In *Proceedings of the 12th USENIX Conference on Operating Systems Design and Implementation*, OSDI, 2016.
- Alvarez, Jose M and Salzmann, Mathieu. Learning the number of neurons in deep networks. In *Proceedings of the 29th International Conference on Neural Information Processing Systems*, NIPS, 2016.
- Bauer, Michael, Treichler, Sean, Slaughter, Elliott, and Aiken, Alex. Legion: Expressing locality and independence with logical regions. In *Proceedings of the International Conference on High Performance Computing, Networking, Storage and Analysis*, 2012.
- Deng, Jia, Dong, Wei, Socher, Richard, Li, Li-Jia, Li, Kai, and Fei-Fei, Li. ImageNet: A large-scale hierarchical image database. In *Proceedings of the IEEE Conference on Computer Vision and Pattern Recognition*, CVPR, 2009.
- Goyal, Priya, Dollár, Piotr, Girshick, Ross B., Noordhuis, Pieter, Wesolowski, Lukasz, Kyrola, Aapo, Tulloch, Andrew, Jia, Yangqing, and He, Kaiming. Accurate, large minibatch SGD: training imagenet in 1 hour. *CoRR*, abs/1706.02677, 2017. URL <http://arxiv.org/abs/1706.02677>.
- Han, Song, Pool, Jeff, Tran, John, and Dally, William J. Learning both weights and connections for efficient neural networks. In *Proceedings of the 28th International Conference on Neural Information Processing Systems*, NIPS, 2015.
- He, Kaiming, Zhang, Xiangyu, Ren, Shaoqing, and Sun, Jian. Deep residual learning for image recognition. In *Proceedings of the IEEE Conference on Computer Vision and Pattern Recognition*, CVPR, 2016.
- Kim, Juyong, Park, Yookoon, Kim, Gunhee, and Hwang, Sung Ju. SplitNet: Learning to semantically split deep networks for parameter reduction and model parallelization. In *Proceedings of the 34th International Conference on Machine Learning*, ICML, 2017.
- Krizhevsky, Alex. One weird trick for parallelizing convolutional neural networks. *CoRR*, abs/1404.5997, 2014. URL <http://arxiv.org/abs/1404.5997>.
- Krizhevsky, Alex, Sutskever, Ilya, and Hinton, Geoffrey E. ImageNet classification with deep convolutional neural networks. In *Proceedings of the 25th International Conference on Neural Information Processing Systems*, NIPS, 2012.
- Lawrence, Steve, Giles, C Lee, Tsoi, Ah Chung, and Back, Andrew D. Face recognition: A convolutional neural-network approach. *IEEE transactions on neural networks*, 1997.
- Mirhoseini, Azalia, Pham, Hieu, Le, Quoc V, Steiner, Benoit, Larsen, Rasmus, Zhou, Yuefeng, Kumar, Naveen, Norouzi, Mohammad, Bengio, Samy, and Dean, Jeff. Device placement optimization with reinforcement learning. 2017.
- Silver, David, Huang, Aja, Maddison, Chris J, Guez, Arthur, Sifre, Laurent, Van Den Driessche, George, Schrittwieser, Julian, Antonoglou, Ioannis, Panneershelvam, Veda, Lanctot, Marc, et al. Mastering the game of go with deep neural networks and tree search. *Nature*, 529:484–489, 2016.
- Simonyan, Karen and Zisserman, Andrew. Very deep convolutional networks for large-scale image recognition. *CoRR*, abs/1409.1556, 2014. URL <http://arxiv.org/abs/1409.1556>.
- Szegedy, Christian, Liu, Wei, Jia, Yangqing, Sermanet, Pierre, Reed, Scott E., Anguelov, Dragomir, Erhan, Dumitru, Vanhoucke, Vincent, and Rabinovich, Andrew. Going deeper with convolutions. *CoRR*, abs/1409.4842, 2014. URL <http://arxiv.org/abs/1409.4842>.
- Szegedy, Christian, Vanhoucke, Vincent, Ioffe, Sergey, Shlens, Jon, and Wojna, Zbigniew. Rethinking the inception architecture for computer vision. In *Proceedings of the IEEE Conference on Computer Vision and Pattern Recognition*, 2016.
- Wang, Tao, Wu, David J, Coates, Adam, and Ng, Andrew Y. End-to-end text recognition with convolutional neural networks. In *Proceedings of the 21st International Conference on Pattern Recognition*, ICPR, 2012.
- Zeiler, Matthew D and Fergus, Rob. Visualizing and understanding convolutional networks. In *European conference on computer vision*, 2014.
- Zhang, Hao, Zheng, Zeyu, Xu, Shizhen, Dai, Wei, Ho, Qirong, Liang, Xiaodan, Hu, Zhiting, Wei, Jinliang, Xie, Pengtao, and Xing, Eric P. Poseidon: An efficient communication architecture for distributed deep learning on GPU clusters. In *2017 USENIX Annual Technical Conference (USENIX ATC 17)*, ATC, 2017.